RP Current Trends In Engineering And Technology (e-ISSN: 2583-5491)
Vol. 5, No. 2 (April – June 2026) pp. 45–50

RESEARCH PLATEAU PUBLISHERS

Cite this article: A. Dutta, M. Ahmed, J. Rani P. Borah, B. Buragohain, S. Bhowmik, Numerical study of beeswax composite as phase change material for unmanned aerial vehicle battery, *RP Cur. Tr. Eng. Tech.* **5** (2026) 45–50.

Original Research Article

Numerical study of beeswax composite as phase change material for unmanned aerial vehicle battery

Amandip Dutta*, Musadik Ahmed, Joyshree Rani Parijat Borah, Bornil Buragohain, Sumit Bhowmik

Department of Mechanical Engineering, National Institute of Technology Silchar, Assam 788010, India
*Corresponding author, E-mail: duttaamandip1194@gmail.com

ARTICLE HISTORY
Received: 15 April 2026
Revised: 26 May 2026
Accepted: 27 May 2026
Published: 13 June 2026

KEYWORDS
Battery thermal management system (BTMS); Phase change material; Beeswax; UAV; Conjugate heat transfer; Latent heat buffering; Passive cooling.

ABSTRACT
Lithium-ion battery packs in unmanned aerial vehicles (UAVs) experience significant thermal stress during high-power manoeuvres, which accelerates degradation and narrows operational margins. The current study thus provides a detailed numerical analysis of a passive thermal management architecture that involves a phase change material (PCM) between two layers of aluminium. Results demonstrate that the metal-bounded beeswax layer provides effective latent heat buffering, delaying temperature rise, smoothing spatial gradients, and lowering peak temperatures compared with unprotected and metal-only enclosures. Melting of the beeswax commences during the mission-relevant heating interval and progresses sufficiently to absorb substantial latent energy, after which sensible heating of the molten layer governs the response. The combination of high-conductivity aluminium skins and a bio-derived PCM yields both rapid lateral spreading and temporal buffering, offering a low-complexity, lightweight, and sustainable passive solution for UAV battery thermal management.

1. Introduction

Lithium-ion batteries are widely used as the primary energy source in UAVs owing to their high energy and power densities, excellent round-trip efficiency, and long cycle life. However, their electrochemical performance is highly temperature-dependent. Prolonged operation above approximately 45-50 °C accelerates the growth of the solid-electrolyte interphase, increases internal resistance, promotes gas evolution, and reduces overall safety margins. In compact UAV platforms, these challenges make effective battery thermal management essential, with particular emphasis on limiting peak temperatures. Conventional active thermal management strategies, such as forced air cooling or liquid circulation systems, often introduce additional complexity, noise, weight, and parasitic power consumption, factors that are undesirable in lightweight aerial systems. As a result, passive thermal management techniques, including the use of heat spreaders and phase change materials (PCMs), have gained attention. PCMs are especially effective under pulsed load conditions, as they absorb heat during phase transition, thereby reducing temperature spikes and delaying the onset of critical thermal limits. Extensive research in battery thermal management has demonstrated the effectiveness of PCMs in moderating transient thermal behavior. Verma et al. [1] conducted an early comparative study showing that PCM integration around battery cells can reduce peak temperatures, with performance strongly influenced by the thickness and spatial distribution of the PCM layer. Building on this, Srivastava et al. [2] analyzed PCM-based systems under varying discharge profiles and found that selecting a PCM with a melting range aligned to the battery's operating temperature significantly reduces temperature rise and stabilizes thermal gradients during high-power operation. Jilte et al. [3] further highlighted that incorporating airflow channels between cells can improve heat dissipation, addressing localized hot spots that PCM alone may not adequately manage. Similarly, the review by Lu et al. [4] emphasized that PCM effectiveness is enhanced when combined with improved conduction or convection mechanisms. To overcome the inherently low thermal conductivity of most organic PCMs, several studies have explored composite approaches. Zhao [5] demonstrated that embedding metal foams or expanded graphite within PCMs significantly enhances heat transfer, with metal foam showing superior performance. At the system level, Paciolla and Papurello [6] reported that integrating PCMs with metallic fins reduces both peak temperatures and spatial temperature variations under dynamic loading conditions. In parallel, attention has been directed toward sustainable PCM alternatives such as beeswax. Rashid and Al-Obaidi [7] identified beeswax as a promising candidate due to its melting temperature range, which aligns well with the upper operating limits of lithium-ion batteries. At the pack level, Putra et al. [8] combined beeswax with heat pipe technology and observed notable reductions in peak temperature along with improved thermal uniformity, indicating that beeswax performs effectively when coupled with efficient heat transfer pathways. Despite these advancements, several challenges remain for UAV-specific applications. First, commonly used organic PCMs, including beeswax and paraffin, exhibit low thermal conductivity, which limits the rate of heat transfer and delays phase transition under short-duration, high-power loads typical

of UAV operations. Second, their performance in compact UAV battery enclosures remains insufficiently explored, particularly under strict constraints of weight and volume. Third, many existing studies do not explicitly track the onset and extent of PCM melting, which are critical parameters for evaluating its effectiveness within the limited duration of UAV missions. To address these limitations, the present study investigates a thin aluminium–beeswax–aluminium composite enclosure. The aluminium layers facilitate rapid heat spreading and improve thermal conduction to the beeswax core, thereby enhancing the utilization of latent heat storage. By focusing on a compact and lightweight configuration suitable for UAV integration, this work evaluates the thermal performance of beeswax-based PCM within realistic operational constraints, offering insights into its applicability for aerial platforms.

2. Methodology

The numerical model incorporates electro-thermal heat generation within the battery domain, transient heat conduction through the aluminium and beeswax layers, and convective heat dissipation at the external surface. All solid regions are thermally coupled using a conjugate heat transfer (CHT) approach, ensuring continuity of both temperature and heat flux across material interfaces. The formulation follows an equation-based framework aligned with the solver setup implemented in ANSYS Fluent, enabling consistency between theoretical modelling and computational execution. The simulation is based on a homogenized representation of a 4S2P lithium-ion battery pack, capturing both internal heat generation and external thermal interactions under conditions representative of UAV operation.

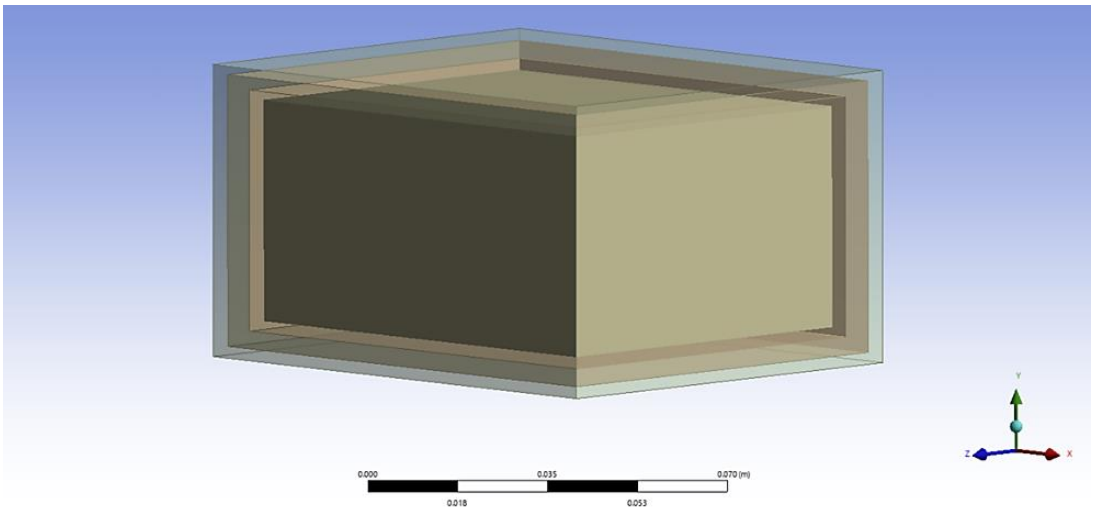

Figure 1: Schematic of the Battery covered with the composite covering: inner Al (2mm)- beeswax (3mm)- outer Al (2mm); outer Al subject to correlation-based convection boundary.

The battery pack, consisting of eight 21700 cells arranged in a 4S2P configuration, is simplified as a single rectangular solid domain. Three configurations are investigated: a bare battery pack, a pack enclosed within a 2 mm aluminium shell, and a composite structure comprising a 2 mm inner aluminium layer, a 3 mm beeswax PCM layer, and a 2 mm outer aluminium layer, as illustrated in Fig. 1. Instead of explicitly modelling the surrounding air domain, convective heat transfer is imposed directly on the outer aluminium surface through an appropriate boundary condition. Gravitational effects are included in the model with a vector of (0, −9.81, 0) m s^{-2}. The energy equation is activated, and the operating pressure is set to 101325 Pa. The computational domain was meshed in ANSYS Mesher using the Prime Mesh algorithm with the Multizone method applied to the aluminium and beeswax regions to capture steep temperature gradients across thin layers. A uniform element size of 1.8×10^{-3} m was selected after grid-independence verification, which showed less than 1% variation in peak temperature with further refinement. The final mesh contained about 109,464 nodes and 387,709 elements, offering a balanced trade-off between accuracy and computational efficiency. The generated grid exhibited good quality (orthogonal quality > 0.85, aspect ratio < 5), ensuring stable and reliable convergence during transient conjugate heat transfer simulations.

Internal electro-thermal heat generation (Bernardi relation) [9]

The pack heat rate $\dot{q}(t)$is the sum of irreversible (Joule) and reversible (entropic) parts:

$$\dot{q}(t) = I(t)^2 R_{pack} + I(t)T \frac{\partial V_{oc,pack}}{\partial T} \quad (1)$$

where $I(t)$ is discharge current [A] (positive on discharge), R_{pack} is pack DC internal resistance [Ω], T is temperature [K], $V_{oc,pack}$ is open-circuit voltage [V], and $\frac{\partial V_{oc,pack}}{\partial T}$ is the pack entropy coefficient [VK^{-1}]. The corresponding volumetric source used in (3) is

$$q'''(t) = \frac{\dot{q}(t)}{V_{pack}} \xrightarrow{peak\ (worst\ case)} q'''_{max} = 9.61 \times 10^4\ W\ m^{-3} \quad (2)$$

with V_{pack} the geometric volume of the homogenized battery block [m^3].

The volumetric heat-generation rate (q'''_{max}) used in the numerical model was obtained from the peak electro-thermal power of the 4S2P battery pack. Based on Bernardi's relation, for a constant load of 350W the combined Joule and entropic heating at the most demanding operating condition yielded a

total pack heat generation of approximately 28W. Considering the volume of eight 21700 cells (2.55×10^{-5} m^3 each) and the pack filling fraction of 0.70 (to account for casing and interstitial voids), this corresponded to an effective volumetric rate of 9.61×10^4 W m^{-3}. This value was applied as a uniform internal source term in the battery domain to represent the worst-case discharge scenario and ensure a conservative estimation of the thermal load during simulation.

Phase change in beeswax (enthalpy formulation)

Latent heat effects in the PCM are captured using the enthalpy method. The transient energy equation expressed in terms of the specific enthalpy h (T) as [9]:

$$\rho \frac{\partial h}{\partial t} = \nabla \cdot (k \nabla T) \quad (3)$$

where $\nabla = \left(\frac{\partial}{\partial x}, \frac{\partial}{\partial y}, \frac{\partial}{\partial z} \right)$ nabla operator is a vector differential operator, ρ is density [kg m^{-3}], k thermal conductivity [W m^{-1} K^{-1}], and T temperature [K]. The specific enthalpy combines sensible and latent heat components [9]:

$$h(T) = h_{ref} + \int_{T_{ref}}^{T} c_p(\theta)\, d\theta + L\, f_\ell(T) \quad (4)$$

where h_{ref} is the reference value of enthalpy, c_p is the specific heat [J kg^{-1} K^{-1}], T is temperature, T_{ref} is the reference temperature, L is the latent heat of fusion [J kg^{-1}], and f_ℓ (T) is the liquid fraction, varying linearly between solidus T_s and liquidus T_ℓ as [10]

$$f_\ell(T) = \begin{cases} 0, & T \le T_s, \\ \frac{T - T_s}{T_l - T_s}, & T_s < T < T_l, \\ 1, & T \ge T_l \end{cases} \quad (5)$$

Conjugate boundary at the outer aluminium surface (convection)

The heat flux normal to the wall equals the convective exchange with the environment [11]:

$$-q_n = -k_{Al} \left. \frac{\partial T}{\partial n} \right|_{wall} = h\,(T_s - T_\infty) \quad (6)$$

where q_n is the outward normal heat flux [W m^{-2}], k_{Al} aluminium thermal conductivity, T_s wall temperature, T_∞ ambient temperature, h the film coefficient [W m^{-2} K^{-1}], and $\frac{\partial}{\partial n}$ the derivative along the outward unit normal $\boldsymbol{n}$. The baseline h is estimated from laminar flat-plate theory over length L [12]:

$$\text{Re}_L = \frac{U_\infty L}{\nu}, \quad \overline{Nu_L} = 0.664\, \text{Re}_L^{\frac{1}{2}}\, \text{Pr}^{\frac{1}{3}}, \quad h = \frac{\overline{Nu_L}\, k_{air}}{L} \quad (7)$$

where Freestream velocity, U_∞ = 1 m s^{-1} , Characteristic Length, L = 0.1008 m, Kinematic Viscosity, ν ~ 1.56×10^{-5} m^2 s^{-1} , Prandtl Number, Pr ~ 0.71, and Thermal Conductivity of air, k_{air} ~ 0.026W m^{-1} K^{-1}, one obtains at $T_\infty = 300K$, $\text{Re}_L \sim 6.46 \times 10^3$, $\overline{Nu_L}$ ~ 47.6, and thus,

$$h = 12.3\, W\, m^{-2}\, K^{-1}. \quad (8)$$

Material Properties Used

All materials were assigned temperature-invariant properties derived from published data.

Table 1 lists the values used for density, specific heat, thermal conductivity, and latent heat where applicable. These inputs ensure consistency with beeswax literature and manufacturer specifications for the 21700 cell and aluminium enclosure.

Table 1: Thermophysical properties used in the numerical model.

Material / Zone	**ρ (kg m^{-3})**	**c_p (J kg^{-1} K^{-1})**	**k (W m^{-1} K^{-1})**	**L (kJ kg^{-1})**	**T_s - T_ℓ (K)**
Aluminium	2719	871	202.4	-	-
Battery	2792	1028	$k_x = k_y$ = 0.9, k_z=24.2	-	-
Beeswax(solid)	1000	2093	0.3	141.5	325-333.6
Beeswax(liquid)	961	2093	0.3	141.5	325-333.6

Overall, the methodology integrates electro-thermal source modelling, phase-change physics, and convection boundary coupling within a unified conjugate framework. Each domain - the battery core, aluminium casing, and PCM layer - interacts thermally through shared interfaces, ensuring energy conservation and accurate transient temperature evolution. This explicit formulation establishes a reproducible and physically grounded simulation workflow for UAV battery thermal management analysis.

3. Results and discussion

The numerical simulations were conducted to evaluate the transient thermal response of the UAV battery module under uniform volumetric heating and identical convective boundary conditions for three distinct configurations: (i) a bare battery pack, (ii) a 2 mm aluminium shell, and (iii) a composite structure comprising 2 mm inner aluminium, 3 mm beeswax PCM, and 2 mm outer aluminium layers. The analysis focuses on comparing temperature evolution, phase-change progression, and thermal uniformity among these configurations to quantify the contribution of the beeswax PCM layer to thermal regulation. Each simulation was executed for 2500 s of discharge, corresponding to the high-power operating phase typical of UAV missions. Figure 2 shows the time evolution of the pack-average temperature for all three battery configurations under the same volumetric heat generation rate ($q'''_{pack} = 9.61 \times 10^4$ Wm^{-3}) and convective boundary condition (h = 12.3W m^{-2} K^{-1}, Eq. (8)). The bare pack exhibits the highest temperature trajectory, reaching 369.6 K at 2500 s. The 2 mm aluminium enclosure reduces this to 363.3 K by enhancing lateral heat spreading and decreasing external resistance. The aluminium-PCM composite (2 mm Al + 3 mm beeswax + 2 mm Al) restricts the rise to 334.2 K, achieving a substantial reduction of 35.4 K compared with the bare case.

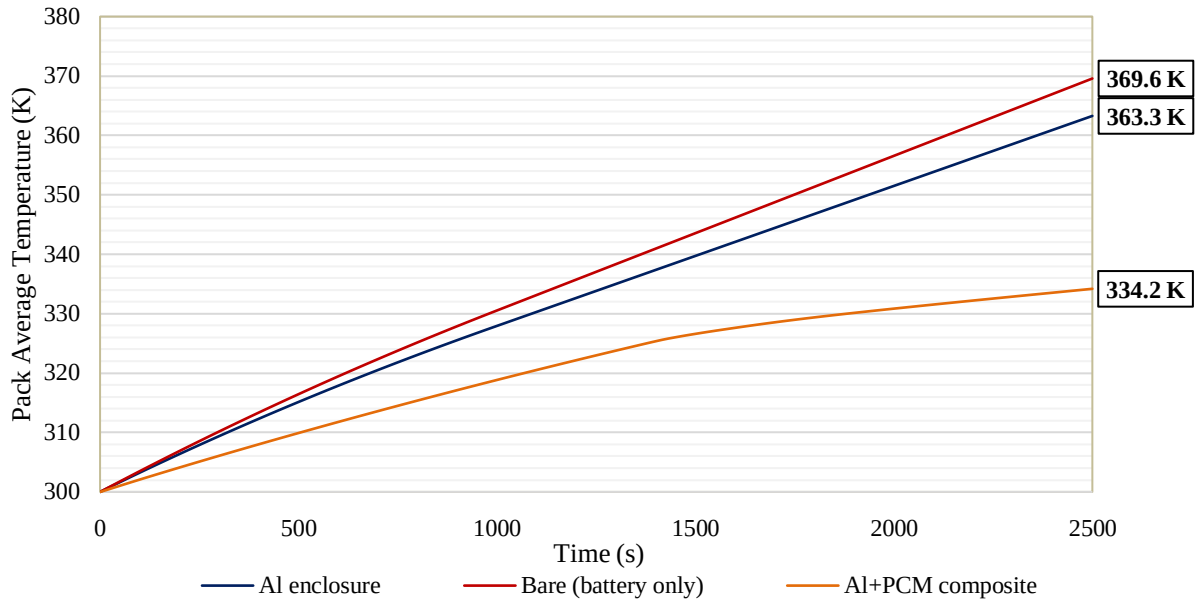

Figure 2: Pack Average Temperature v/s Time for Battery Cooling Configuration. The beeswax melting range (325-333.6 K) is highlighted. End-point temperatures are annotated: bare ~ 369.6K, Al enclosure ~ 363.3K, and Al + PCM composite ~ 334.2K.

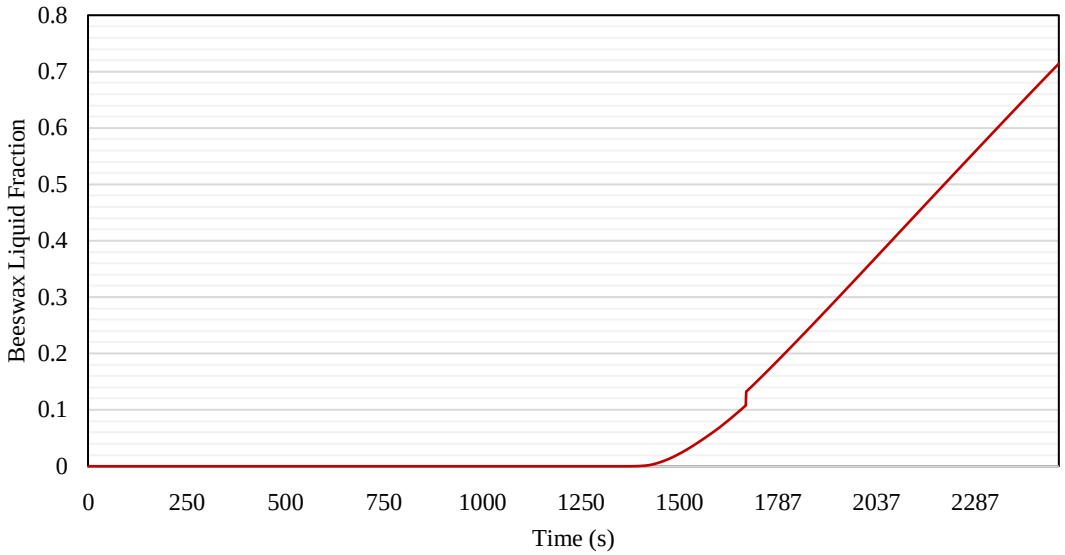

Figure 3: Volume-averaged liquid fraction of beeswax PCM versus time. The onset of melting occurs after ~1400 s, with approximately 80% liquid phase at 2500 s.

Thermal Response and Phase Change Behaviour

The composite configuration exhibits a noticeable change in slope within the temperature band T [325 K, 333.6 K]. This region corresponds to the beeswax melting interval, during which the material absorbs latent heat at nearly constant temperature. The apparent heat capacity, increases significantly, resulting in a smaller rate of temperature rise. Once the PCM becomes fully liquid, the curve reverts to a gentler linear slope corresponding to sensible heating of the molten beeswax and the aluminium skins. This smooth transition confirms that the PCM acts as a thermal buffer, temporarily storing energy that would otherwise raise the cell temperature.

Liquid Fraction Evolution

The temporal variation of the beeswax liquid fraction, shown in Figure 3, provides insight into the extent of phase transition. The PCM remains completely solid until approximately 1400 s, after which melting begins. The liquid fraction increases gradually, reaching about 0.8 by 2500 s. This demonstrates partial melting within the PCM domain, consistent with the moderate temperature rise observed in Figure 2. The delayed onset of melting ensures that latent heat absorption coincides with the critical stage of the pack temperature excursion, thereby delivering maximum benefit during the most thermally stressed period.

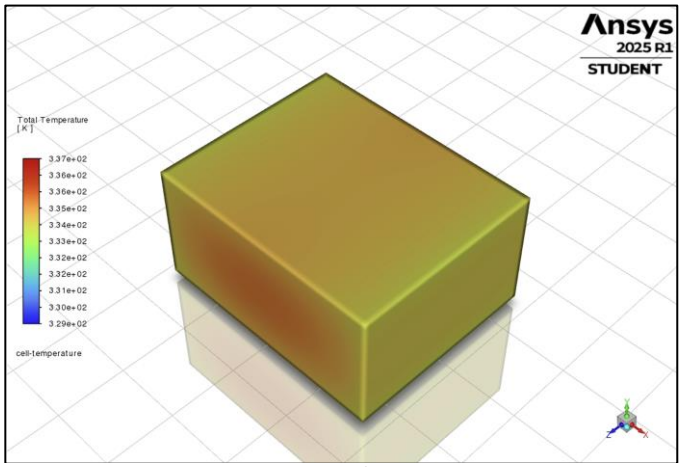

Figure 4: Temperature contour of the composite at t = 2500 s. Maximum temperature is ~337 K.

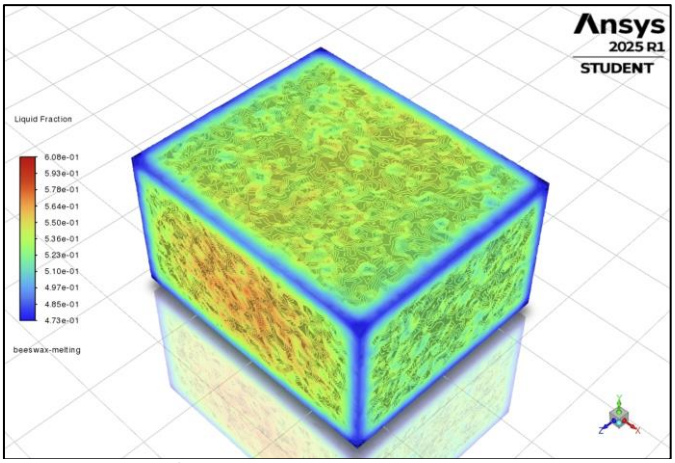

Figure 5: Liquid-fraction contour at t = 2500 s. Melting initiates near the battery-PCM interface and extends outward, achieving an average liquid fraction of ~ 0.6.

Temperature and Melting Distribution at 2500 s

Figure 4 and Figure 5 show the spatial temperature and liquid-fraction fields within the composite at t = 2500 s. The temperature distribution (Figure 4) is nearly uniform, with a maximum near 337 K close to the battery-PCM interface. The outer aluminium layers efficiently spread heat laterally, minimizing temperature gradients across the casing. The corresponding liquid-fraction contour (Figure 5) reveals that melting is nonuniform, beginning near the inner surfaces adjacent to the heat source and propagating outwards. The beeswax near the outer boundary remains partially solid, indicating that thermal conduction and latent storage are well balanced within the given duration.

Quantitative Assessment and Practical Implications

Table 2 compares the steady-state temperatures and dominant mechanisms for each configuration. The Al-only enclosure provides modest improvement through heat spreading, whereas the Al+PCM composite delivers a significantly higher reduction due to latent heat storage and enhanced thermal inertia. The combination of aluminium's high conductivity and beeswax's phase-change capacity establishes both spatial and temporal control of the temperature field. The PCM engages only after the pack approaches ~ 325 K, indicating an adaptive, self-regulating response ideal for UAV missions with intermittent power surges. Overall, the simulation confirms that beeswax-based PCMs, even with modest thermal conductivity, significantly delay temperature rise by absorbing heat during the melting phase. The aluminium skins ensure mechanical containment and thermal uniformity, making the Al-beeswax-Al structure a robust and lightweight passive thermal-management solution for UAV battery systems.

Table 2: Thermal performance at t = 2500 s under $q'''_{pack} = 9.61 \times 10^4\ W\ m^{-3}$ and $h = 12.3\ Wm^{-2}K^{-1}$.

Configuration	Peak Temperature (K)	Reduction vs. Bare Pack (K)	Dominant Mechanism
Bare pack	369.6	-	Conduction to air film
2 mm Aluminium enclosure	363.3	6.3	Lateral spreading + convection
Al + 3 mm PCM + Al (sandwiched)	334.2	35.4	Spreading + latent-heat buffering

4. Conclusions

This study presented a streamlined ANSYS Fluent-based framework to evaluate the thermal benefits of integrating a thin beeswax PCM layer between aluminium skins for a compact UAV battery pack. The results confirm that the aluminium-beeswax-aluminium structure substantially improves heat management compared to a bare battery and an aluminium-only enclosure. The beeswax provides effective transient thermal buffering through its sensible and latent heat capacity, while the aluminium layers enhance lateral heat spreading and promote faster heat rejection to the environment. The combined effect is a slower and more controlled temperature rise, along with a noticeably lower peak battery temperature under identical operating conditions. This behaviour is particularly advantageous for UAV applications, where batteries experience intermittent high-power loads that typically drive rapid thermal excursions. The proposed architecture achieves these improvements with minimal added complexity and without significant weight or volume penalties. Overall, the aluminium-beeswax-aluminium configuration demonstrates a practical and sustainable approach to enhancing battery thermal stability. Its simplicity, effectiveness, and compatibility with compact UAV platforms make it a promising candidate for next-generation battery thermal management solutions.

Authors' contributions

All authors contributed equally to the conception, design, experimental work, data analysis, interpretation of results, and preparation of the manuscript. All authors reviewed and approved the final version of the manuscript for publication.

Conflicts of interest

The author declares no conflict of interest.

Funding

This research received no external funding.

Data availability

No new data were created.

References

[1] A. Verma, S. Shashidhara, D. Rakshit, A comparative study on battery thermal management using phase change material (PCM), *Therm. Sci. Eng. Prog*. **11** (2019) 74–83.

[2] G. Srivastava, R. Nandan, M.K. Das, Thermal runaway management of Li-ion battery using PCM: A parametric study, *Energy Convers. Manag. X* **16** (2022) 100306.

[3] R.D. Jilte, V.S. Kanse, A.R. Pathak, S.C. Kamate, P.V. Walke, Battery thermal management system employing phase change material with cell-to-cell air cooling, *Appl. Therm. Eng.* **149** (2019) 1076–1086.

[4] M. Lu, X. Zhang, J. Ji, X. Xu, Y. Zhang, Research progress on power battery cooling technology for electric vehicles, *J. Energy Storage* **27** (2020) 101155.

[5] C.Y. Zhao, Heat transfer enhancement of high temperature thermal energy storage using metal foams and expanded graphite, *Sol. Energy Mater. Sol. Cells* **95** (2011) 636–643.

[6] P. Paciolla, D. Papurello, Improved thermal management of Li-Ion batteries with phase-change materials and metal fins, *Batteries* **10** (2024) 310.

[7] F.L. Rashid, M.A. Al-Obaidi, Recent innovations and developments concerning beeswax as phase change material for thermal energy storage: A review, *J. Therm. Anal. Calorim.* **148** (2023) 12859–12876.

[8] N. Putra, R. Roekettino, A. Suparman, Y. Yuliarto, Y. Kim, Performance of beeswax PCM and heat pipe as passive battery cooling system for electric vehicles, *Case Stud. Therm. Eng.* **21** (2020) 100655.

[9] D.K. Mishra, S. Bhowmik, K.M. Pandey, Numerical investigation of beeswax-based phase change material for thermal management of Li-ion battery, *Mater. Today Proc*. **45** (2021) 6527–6532.

[10] S. Alam, J. Das, S. Bhowmik, Thermal performance analysis of copper foam enhanced beeswax composite with varying porosity as phase change material for thermal management of Li-ion battery, *Phys. Scr*. **100** (2025) 085967.

[11] A. Bejan, Convection Heat Transfer, 4th edn., Wiley, Hoboken, NJ (2013).

[12] Y.A. Çengel, A.J. Ghajar, Heat and Mass Transfer: Fundamentals and Applications, 5th edn., McGraw-Hill, New York, NY (2015).